Thermoelectric Power Sensor for Microwave Applications by Commercial CMOS Fabrication

Veljko Milanović, Michael Gaitan, Edwin D. Bowen, Nim H. Tea, and Mona E. Zaghloul

***Abstract*—This letter describes an implementation of a thermoelectric microwave power sensor fabricated through commercial CMOS process with additional maskless etching. The sensor combines micromachined coplanar waveguide and contact pads, a microwave termination which dissipates heat proportionally to input microwave power, and many aluminum-polysilicon thermocouples. The device was designed and fabricated in standard CMOS technology, including the appropriate superimposed dielectric openings for post-fabrication micromachining. By removing the bulk silicon located beneath the device through micromachining, thermal and electromagnetic losses are minimized. The sensor measures signal true rms power in the frequency range up to 20 GHz with input power in the -30 dBm to $+10$ dBm range. Over this 40 dB dynamic range, output voltage versus input power is linear within less than $\pm 0.16\%$. Automatic network analyzer data show an acceptable input return loss of less than -30 dB over the entire frequency range.**

I. Introduction

THERMOCOUPLE-BASED power sensors have been one of the most widely used tools for microwave power measurement [1]. These sensors employ a simple principle of rf power to thermal power conversion which is then indirectly measured. In microwave applications, a matched terminating resistor dissipates the rf energy as heat that is converted into dc voltage by one or more thermocouples [2], thus providing an accurate measurement of true rms power absorbed by the resistor.

Standard CMOS technology cannot be used for microwave applications because of the lossy nature of silicon substrate at microwave frequencies [3], [4]. Currents induced in the substrate due to electromagnetic coupling result in unwanted frequency-dependent losses and dispersive characteristics. At the same time, standard CMOS integrated circuit technology is not suitable for the design of thermoelectric devices, such as thermocouples, due to the strong thermal coupling of devices to the silicon substrate, making such sensors intolerably inefficient.

In order to reduce these inefficiencies, it is of interest to remove the silicon substrate from directly beneath the thermal and microwave structures, while still allowing the monolithic integration of CMOS electronics. To achieve this, we have used a post-processing procedure involving recently developed methods of maskless micromachining of CMOS integrated circuits [5].

Micromachining techniques are becoming increasingly popular for high-frequency applications [4], [6]–[12]. At the same time, silicon micromachining techniques have also been applied to CMOS technology in order to make a variety of thermo-electro-mechanical structures. Thermoelectric power sensors fabricated in CMOS technology have been reported for device structures operated below 1 GHz [11], [12]. In this work we report on CMOS implementation of thermoelectric microwave power sensors which operate efficiently up to 20 GHz, and are expected to operate at higher frequencies.

Our implementation of this device structure in a commercial CMOS process results in the provision of monolithic integration of detection and output circuitry with the power sensor on a single chip. We have found that there is a trade-off with slightly reduced accuracy because the conductive and resistive films available in the CMOS fabrication process, aluminum and polysilicon, may not be optimal for the application. However, the capability of fabricating this structure in CMOS technology could have a significant economic advantage as a low-cost microwave power sensor with integrated electronics where some loss in accuracy is acceptable.

II. Theory of Operation

The proposed new type of micromachined thermoelectric converter (thermo-pile) is comprised of a new arrangement of transmission lines, resistive terminations, and thermocouple contacts, all of which are formed with the standard CMOS process layers. The design includes *open* areas [5] which are superimposed dielectric openings, designed to expose the silicon substrate for post-fabrication micromachining. Micromachining selectively removes silicon in the vicinity of the microwave and thermocouple devices. A microphotograph of the micromachined thermoelectric converter is shown in Fig. 1. A low-loss 50 Ω micromachined coplanar waveguide (CPW) transmission line, that we recently reported [4], provides the input connection to the matched resistive load which converts the incident rf energy into heat. The accurately matched resistive load is formed by a distributed network tee-transmission line as shown. The characteristic impedance of the transmission lines in each of the distributed arms of the tee is 100 Ω. The resistive value of the center conductor in each arm of the tee is also 100 Ω at dc. The net input impedance

Manuscript received January 23, 1997; revised May 14, 1997. This work was supported by the Naval Command, Control and Ocean Surveillance Center, RDT&E DIV, San Diego, CA. The work of V. Milanović was supported by RF Microsystems, San Diego, CA. The work of N. H. Tea was supported by the National Research Council Postdoctoral Fellowship Program.

V. Milanović and M. E. Zaghloul are with the Department of Electrical Engineering and Computer Science, The George Washington University, Washington, DC 20052 USA.

M. Gaitan and N. H. Tea are with Semiconductor Electronics Division, National Institute of Standards and Technology, Gaithersburg, MD 20899 USA.

E. D. Bowen is with RF Microsystems, Inc., San Diego, CA 92123 USA.

Publisher Item Identifier S 0741-3106(97)06686-X.

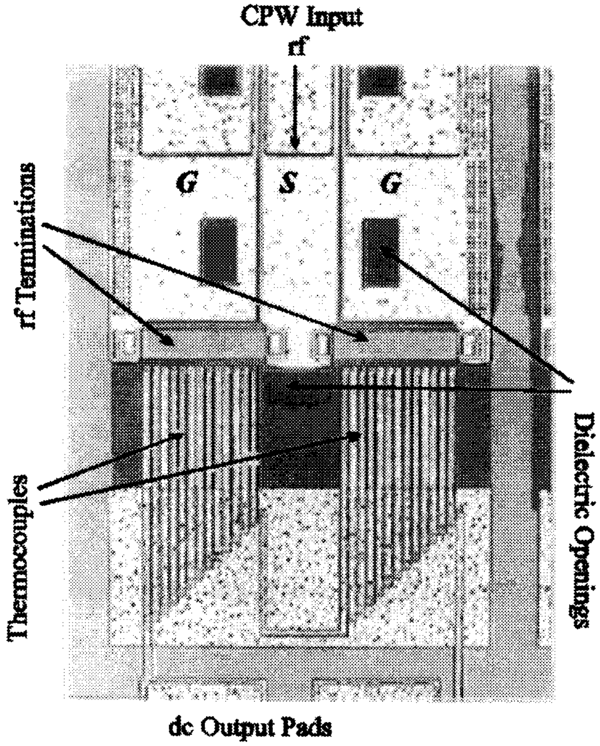

Fig. 1. Microphotograph of the new CMOS-compatible thermoelectric sensor (GSG = Ground-Signal-Ground).

of the complete thermoelectric sensor assembly as seen by a CPW source is therefore 50 Ω, as desired.

Fig. 1 also shows a set of closely spaced thermocouple junctions located on the bottom side of the rf-heated resistive elements of the rf terminations. Each of these hot junctions is in series with a cold junction located above the base silicon material. To better stabilize the temperature of the cold junctions to that of the ensemble, the aluminum-polysilicon contacts of the cold junctions are covered with second-layer metal. There are altogether 26 thermocouples connected in series to increase the output voltage signal. Thus, the thermoelectric sensor efficiently converts rf electrical energy to an output dc voltage.

The time constant for power measurements is on the order of milliseconds. This is due to the miniature dimensions of the device and very small heat capacity of the assembly. The short thermal time-constants of the sensor allow for measurements of time-varying signals such as pulsed waveforms with envelope frequencies up to several kHz.

III. Sensor Fabrication and Measurement Setup

Test chips were fabricated in a double-poly 2-μm CMOS n-well process through the MOSIS service [5], and were subsequently etched in our laboratory. As shown in Fig. 1, the *open* areas are on both sides of the transmission lines and resistors. Since there is no overlap of the two *open* areas, anisotropic etch would not result in suspended structures, but would instead form many separate etch pits. For this reason, we combined two types of etches, as we previously reported [4]. In the first step, a gaseous isotropic etchant, xenondifloride

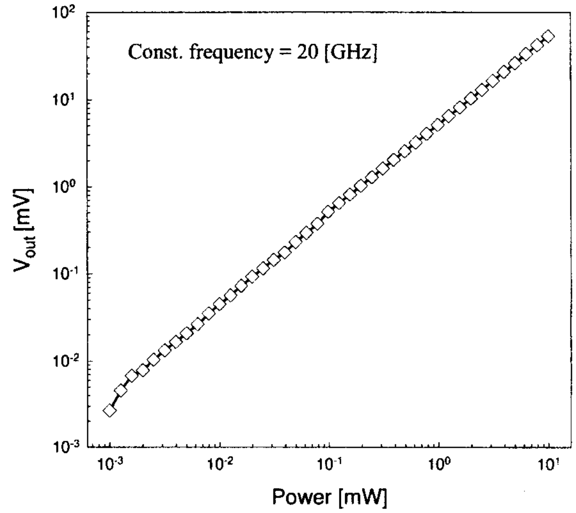

Fig. 2. Measured rf-power versus output dc voltage conversion.

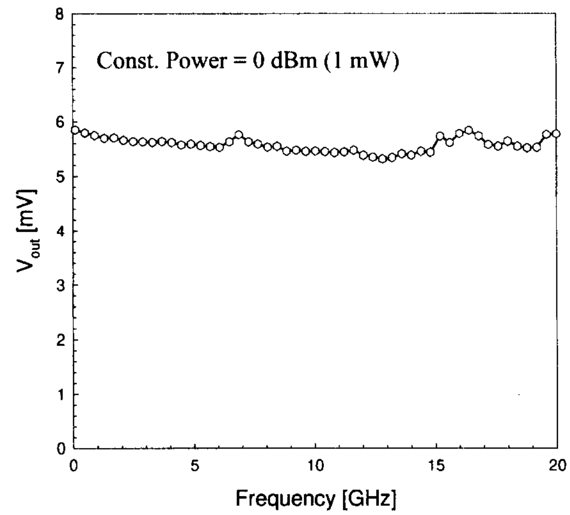

Fig. 3. Measured frequency versus output voltage characteristics.

[13] is used. After approximately 8 min (16 30-s pulses) pits that form on each side of the resistors or transmission lines, connect with each other beneath the structure, at which point anisotropic etching can be successfully applied. For the second etch, chips are placed into an anisotropic etchant, ethylenediamine-pyrocatechol water (EDP). The EDP etch takes approximately 45 min at 92 °C. The resulting devices are adequately thermally and electromagnetically isolated from the substrate.

Measurements were performed at frequencies from 50 MHz up to 20 GHz using an HP8510C[1] automatic network analyzer, microwave probes, and an accurate digital voltmeter. To test the linearity of the device, signals with power from −30 dBm to 10 dBm (1 μW to 10 mW) at 20 GHz were applied at the input, and output dc voltages were recorded. These measurements are shown in Fig. 2. The frequency dependence of the sensors was similarly recorded while sweeping the

[1] Certain commercial products are identified in this paper to specify the procedure adequately. This does not imply recommendation or endorsement by NIST, nor does it imply that those commercial products are the best available for the purpose.

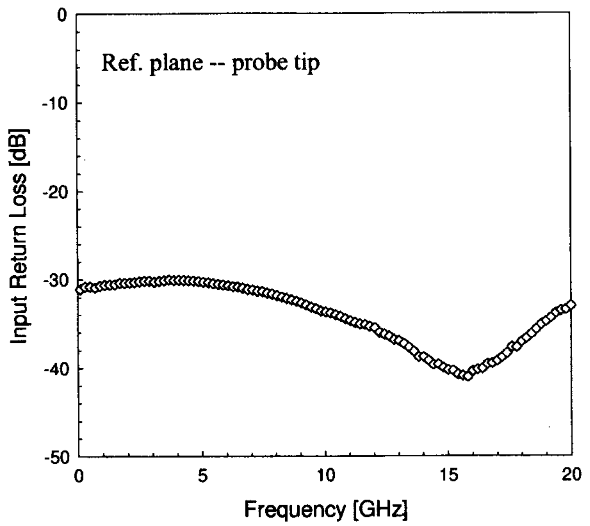

Fig. 4. Measured input return loss characteristics of the rf input of the detector.

input frequency, at constant power of 0 dBm (1 mW). The results are given in Fig. 3. Another important measurement is that of the input mismatch error of the device over the entire frequency range. The mismatch is determined from the measured s_{11} parameters of the rf input. The reference plane for the measurement was the probe tip, and so the results include parasitic effects of the pads and underlying substrate. Nevertheless, the input mismatch error for both devices measured below -30 dB over the entire frequency range. Input reflection measurements of the novel sensor device are shown in Fig. 4.

IV. Discussion of the Results

Measurements have shown that the sensors have very good rf-dc linearity. As shown in Fig. 2, in a log-log plot, the input power to output voltage relationship is quite linear throughout the 40 dB input range for both devices. A $\pm 0.16\%$ linearity error was calculated from the measured data. The slope of the graph is (5.32 ± 0.0016) mV/mW, which is an acceptable sensitivity, provided by the large number of Al-polysilicon thermocouple junctions with relatively high Seebeck coefficient. The frequency response shown in Fig. 3 is relatively flat up to 20 GHz. Although the coplanar waveguide and the thermoelectric sensor are suspended away from the silicon substrate, the rf input pads remain over the substrate which results in some frequency dependence that cannot be neglected. Etching a larger pit under the device would certainly improve the frequency characteristics. It becomes very difficult to perform accurate measurements, however, when the contacts pads are partially or fully suspended. In a practical device, these issues will be solved by bonding or other methods which would allow the entire rf circuit to be fully suspended.

The input mismatch measurements in Fig. 4 show desirable mismatch error below -30 dB at all frequencies. The s_{11} measurements were performed with probe tip calibration, including the parasitics in the probing pads. It is expected that the actual input return loss in devices without pads would be lower.

V. Conclusion

We have reported a novel configuration thermoelectric power sensor for microwave applications. The sensor was fabricated in CMOS technology with additional maskless post-processing. The sensor is based on traditional thermal converter measurement techniques, and optimized for microwave frequencies. The device shows good linearity characteristics, and low return loss up to 20 GHz. The CMOS implementation gives the advantages of low cost and easy integration with CMOS circuits.

Acknowledgment

The authors wish to thank J. Suehle for many technical discussions and use of various laboratory equipment.

References

[1] J. R. Kinard, J. R. Hastings, T. E. Lipe, and C. B. Childers, *AC–DC Difference Calibration*, NIST Special Publ., NIST SP 250-27, 1989.
[2] Hewlett Packard Co., "Fundamentals of RF and microwave power measurement," *Appl. Note AN 64-1*, 1978.
[3] S. Zaage and E. Grotelueschen, "Characterization of the broadband transmission behavior of interconnections on silicon substrates," *IEEE Trans. Comp. Hybrids, Manufact. Technol.*, vol. 16, pp. 686–691, Nov. 1993.
[4] V. Milanović, M. Gaitan, E. D. Bowen, and M. E. Zaghloul, "Micromachined microwave transmission lines in CMOS technology," *IEEE Trans. Microwave Theory Tech.*, vol. 45, pp. 630–635, May 1997.
[5] N. H. Tea, V. Milanović, C. A. Zincke, J. S. Suehle, M. Gaitan, M. E. Zaghloul, and J. Geist, to be published.
[6] L. P. B. Katehi, G. M. Rebeiz, T. M. Weller, R. F. Drayton, H.-J. Cheng, and J. F. Whitaker, "Micromachined circuits for millimeter- and submillimeter-wave applications," *IEEE Trans. Antennas Propagat.*, vol. 35, pp. 9–17, Oct. 1993.
[7] W. R. McGrath, C. Walker, M. Yap, and Y.-C. Tai, "Silicon micromachined waveguides for millimeter-wave and submillimeter-wave frequencies," *IEEE Microwave Guided Wave Lett.*, vol. 3, pp. 61–63, Mar. 1993.
[8] J. Y.-C. Chang, A. A. Abidi, and M. Gaitan, "Large suspended inductors on silicon and their use in a 2-μm CMOS RF amplifier," *IEEE Electron Device Lett.*, vol. 14, May 1993.
[9] V. Milanović, M. Gaitan, and M. Zaghloul, "Micromachined thermocouple microwave detector in CMOS technology," in *Proc. Midwest Symp. Circuits and Systems*, Ames, IA, Aug. 1996, vol. 1, pp. 273–276.
[10] P. Kopystynski, E. Obermeier, H. Delfs, and A. Loser, "Silicon power microsensor with frequency range from DC to microwave," in *6th Int. Conf. Solid-State Sensors and Actuators Tech. Dig. (Transducers '91)*, San Francisco, CA, June 1991, pp. 623–626.
[11] D. Jaeggi and H. Baltes, "Thermoelectric AC power sensor by CMOS technology," *IEEE Electron Device Lett.*, vol. 13, July 1992.
[12] M. Gaitan, J. Kinard, and D. X. Huang, "Performance of commercial CMOS foundry-compatible multijunction thermal converters," in *7th Int. Conf, Solid-State Sensors and Actuators Tech. Dig. (Transducers '93)*, Yokohama, Japan, 1993, pp. 1012–1014.
[13] F. I.-J. Chang, R. Yeh, G. Lin, P. B. Chu, E. Hoffman, E. J. J. Kruglick, and K. S. J. Pister, "Gas-phase silicon micromachining with Xenon Difluoride," in *SPIE 1995 Symp. Micromachining and Microfab.*, Austin, TX, 1995, pp. 117–128.